ISSN 1070-4280, Russian Journal of Organic Chemistry, 2020, Vol. 56, No. 7, pp. 1258–1271. © Pleiades Publishing, Ltd., 2020.

Structure Determination and Quantum Chemical Analysis of 1,3-Dipolar Cycloaddition of Nitrile Imines and New Dipolarophiles and POM Analyses of the Products as Potential Breast Cancer Inhibitors

T. A. Farghaly[a,b,*], I. M. Abbas[a], W. M. I. Hassan[a,c], M. S. Lotfy[a], N. T. Al-Qurashi[d], and T. Ben Hadda[e]

[a] *Department of Chemistry, Faculty of Science, Cairo University, Giza, 12613 Egypt*

[b] *Department of Chemistry, Faculty of Applied Science, Umm Al-Qura University, Makkah Almukkarramah, 21514 Saudi Arabia*

[c] *Chemistry Department, Faculty of Science, King Abdulaziz University, Jeddah, 21589 Saudi Arabia*

[d] *Department of Basic Science, University College in Adam, Umm Al-Qura University, Makkah Almukkarramah, 21514 Saudi Arabia*

[e] *Laboratoire Chimie Matériaux, FSO, Université Mohammed 1ER, Oujda, 60000 Morocco*

**e-mail: thoraya-f@hotmail.com; tamohamed@uqu.edu.sa*

Received January 31, 2020; revised February 12, 2020; accepted February 18, 2020

Abstract—The 1,3-dipolar cycloaddition of nitrile imines to 11-aryl-4-(arylmethylidene)-1,2,3,4,11,11a-hexahydrodibenzo[*b*,*e*][1,4]thiazepines possessing exocyclic C=C and endocyclic C=N bonds as dipolarophilic sites showed site selectivity, depending on the type of C-substituent in the nitrile imine. 1,3-Dipolar cycloaddition of *C*-aryl nitrile imines occurred selectively to the exocyclic C=C bond, whereas the endocyclic C=N bond was involved in the cycloaddition with *C*-ethoxycarbonyl nitrile imines. A combination of total energy and molecular orbital plots for the highest occupied and lowest unoccupied molecular orbitals was used to verify the proposed reaction mechanisms and stereoselectivity. Some of the isolated products exhibited moderate to good antitumor activity. The results of POM analysis of the relative cytotoxicity of these new derivatives in comparison to Doxorubicin are also reported.

Keywords: hydrazonoyl chlorides, site selectivity, regioselectivity, antitumor activity, pharmacophore sites, Petra/Osiris/Molinspiration (POM) analyses

DOI: 10.1134/S1070428020070210

INTRODUCTION

In recent years, chemoselectivity in 1,3-dipolar cycloadditions of nitrile imines to multifunctional dipolarophiles possessing two or more different dipolarophilic sites has attracted the interest of several research groups [1]. For example, the cycloaddition of nitrile imines to compounds **I** and **II** (Fig. 1) which contain exocyclic C=C and endocyclic C=N double bonds was found to occur selectively to the exocyclic C=C double bond to give the corresponding spiro pyrazole derivative [2, 3]. Contrary to the foregoing reports, it was found that the cycloaddition of nitrile imines to **III** and **IV** (Fig. 1) occurred selectively to the endocyclic C=N double bond to yield fused 1,2,4-triazoles [4, 5]. Both spiro pyrazoles and fused 1,2,4-triazoles have been reported to exhibit a wide range of biological activities [6, 7].

Quantum chemical calculations play an important role in elucidation and confirmation of the actual structure of heterocyclic compounds and stereoselectivity of the reactions. In this article, we deeply investigated the reasons behind preferences of one mechanism over the other by density functional theory (DFT) calculations.

Guided by the above-mentioned findings and continuing our studies on nitrile imine precursors [8–16], we thought it interesting to explore the site selectivity

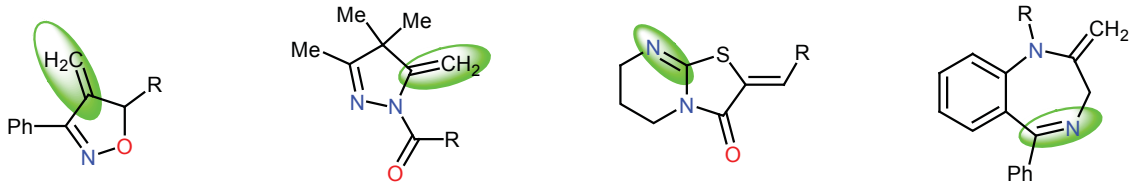

I II III IV

Fig. 1. Structures of compounds **I**–**IV**.

in the cycloaddition of nitrile imines to 11-aryl-4-(arylmethylidene)-1,2,3,4,11,11a-hexahydrodibenzo[*b*,*e*][1,4]thiazepines **3** (Scheme 1) which possess two dipolarophilic sites, namely the exocyclic C=C and endocyclic C=N double bonds. In addition, the cycloaddition products seemed promising for studying their in vitro antitumor activity.

RESULTS AND DISCUSSION

The required bifunctional dipolarophiles **3** were prepared by refluxing an equimolar mixture of 2,6-bis-(arylmethylidene)cyclohexan-1-ones **1a** and **1b** with 2-aminobenzenethiol (**2**) in ethanol in the presence of acetic acid. On the basis of spectroscopic and elemental analyses data, the isolated compounds proved to have structure **3** while structure **4** was discarded. For example, the ^{1}H NMR spectra of **3**, apart from signals of the aromatic protons and the three CH_2 groups, showed one doublet at δ 5.05 ppm (1H, J = 12.6 Hz, 11-H) and a multiplet signal near δ 3.00 ppm (1H, 11a-H). The large coupling constant J = 12.6 Hz indicated *E* configuration of the exocyclic C=C double bond. Table 1 contains the total energies (E_{tot}), HOMO and LUMO energies (E_{HOMO}, E_{LUMO}), and dipole moments (μ) of all possible products and reactants in all possible pathways of the proposed mechanisms. For the reaction between **1** and **2** to form either **3** or **4**, the total energy of **3** is less than that of **4** by 6.28 kcal/mol. The dipole moment and energy gap of **3** are comparable to those of initial compound **1**. Molecule **4** has the highest dipole moment among **1**–**4**. Compound **2** has a higher band gap than compounds **1**, **3**, and **4** which are characterized by comparable values. Higher band gap usually indicates lower reactivity which leads to the conclusion that the reaction is mainly driven by the high reactivity of **1**.

Compounds **3a** and **3b** were reacted with *C*,*N*-diaryl nitrile imines **6** generated in situ from the corresponding hydrazonoyl halides **5** by the action of triethylamine in benzene under reflux. In each case, only one pure product was formed (according to the data of TLC monitoring). These findings indicated that the described reaction is chemo- and regioselective. Theoretically, the addition of nitrile imines **6** to compounds **3** could lead to the formation of four isomeric cycloadducts **7**–**10** (Scheme 2). The isolated compounds were assigned structure **7** on the basis of spectroscopic

Scheme 1.

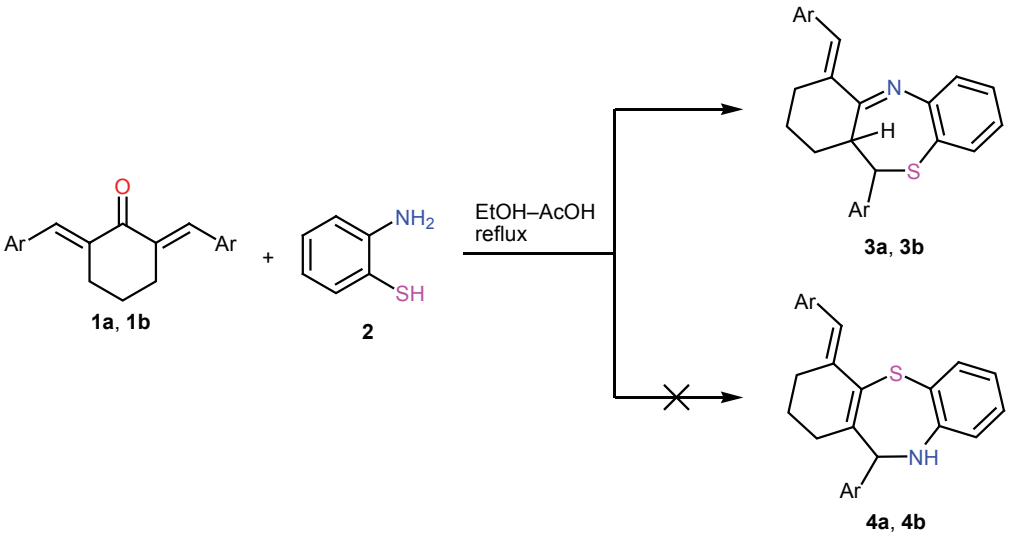

Ar = 4-ClC_6H_4 (**a**), 4-FC_6H_4 (**b**).

Scheme 2.

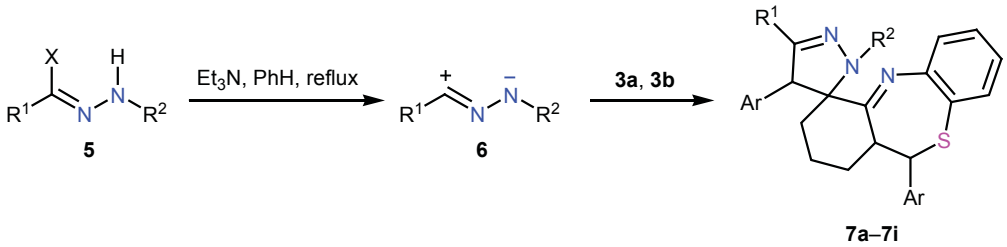

7, Ar = 4-ClC_6H_4 (**a**–**d**), 4-FC_6H_4 (**e**–**i**); R^1 = Ph (**a**, **c**, **e**, **g**), 4-ClC_6H_4 (**b**, **f**), thiophen-2-yl (**d**, **h**), furan-2-yl (**i**); R^2 = Ph (**a**, **b**, **e**, **g**), 4-$O_2NC_6H_4$ (**c**, **d**, **g**–**i**).

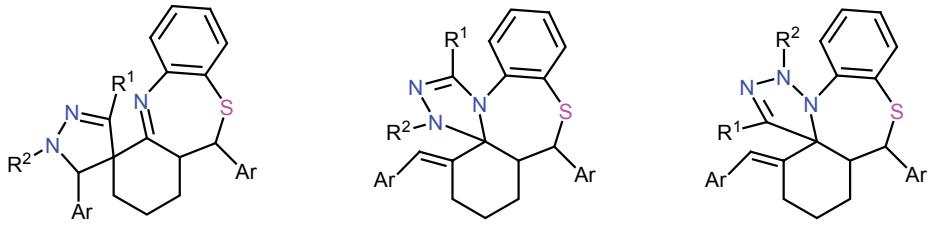

data (see Experimental). In addition to signals of aromatic protons, three CH_2 groups, 11-H, and 11a-H, the ^{1}H NMR spectra of **7a**–**7i** showed a singlet of 4′-H (dihydropyrazole ring) in the region δ 5.4–5.6 ppm. The position of the latter signal is in agreement with published data for structurally related dihydropyrazoles, whereas proton in the 5-position of dihydropyrazoles usually resonates at a lower field (δ > 5.6 ppm)[17, 18].

The formation of compounds **7** rather than **8**–**10** was also confirmed by theoretical calculations. The total energies of **7** and **8** are lower than those of **9** and **10** by at least 27 kcal/mol. The energy of the reaction calculated by subtracting the sum of the energies of the reactants (compounds **3** and **6**) from the energy of the product (compound **7** or **8**) was 32.86 and 34.76 kcal×mol^{-1} for the formation of **7** and **8**, respectively. Thus, the difference is only ~5.7%. This small energy difference cannot be regarded as strong evidence in favor of one or another pathway. The molecular orbital plot was utilized as the best way for explanation the

Table 1. The total energy E_{tot}, energies of HOMO, LUMO, energy gaps ΔE, and dipole moments μ of structures **1**–**16**

Compound no.	E_{tot}, a.u.	E_{HOMO}, a.u.	E_{LUMO}, a.u.	$\Delta E = E_{LUMO} - E_{HOMO}$, eV	μ, D
1	–1767.6358245	–0.24149	–0.09794	3.9062	2.3527
2	–685.9041914	–0.21866	–0.02600	5.2426	1.6466
3	–2377.0712272	–0.22014	–0.07711	3.8921	2.2437
4	–2377.06367821	–0.20779	–0.06611	3.8554	3.4511
5	–1071.8705179	–0.20898	–0.06355	3.9573	0.1292
6	–610.9791641	–0.19603	–0.06757	3.4956	3.7489
7	–2988.1027573	–0.19713	–0.06531	3.587	1.9552
8	–2988.1057806	–0.20064	–0.06574	3.6708	3.2950
9	–2988.0362443	–0.20315	–0.05958	3.9067	3.4204
10	–2988.0597733	–0.20590	–0.06135	3.9334	2.3903
11	–1147.3520943	–0.21941	–0.06853	4.1057	1.6649
12	–686.45938155	–0.21550	–0.07329	3.8698	1.1466
13	–3024.2621630	–0.21934	–0.06763	4.1283	4.0006
14	–3024.2701903	–0.21761	–0.07615	3.8494	3.3918
15	–3024.2140216	–0.21467	–0.06576	4.0521	4.3520
16	–3024.1990399	–0.21458	–0.06513	4.0668	2.4407

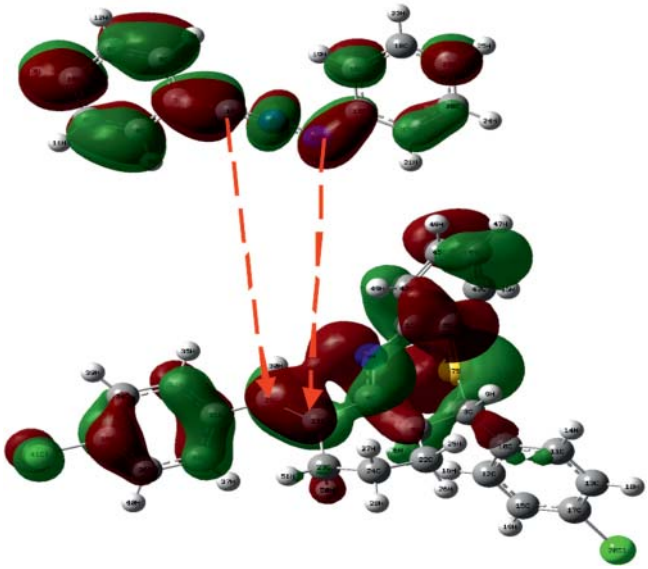

Fig. 2. Molecular orbital plot for the LUMO of compound **6** (above) and HOMO of **3** (below) in the orientation to form compound **7**.

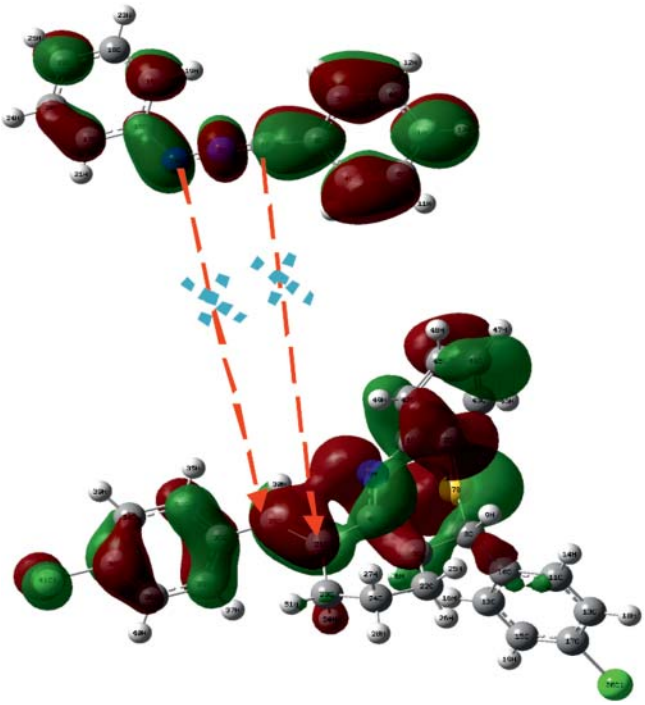

Fig. 3. Molecular orbital plot for the LUMO of compound **6** (above) and HOMO of **3** (below) in the orientation to form compound **8**.

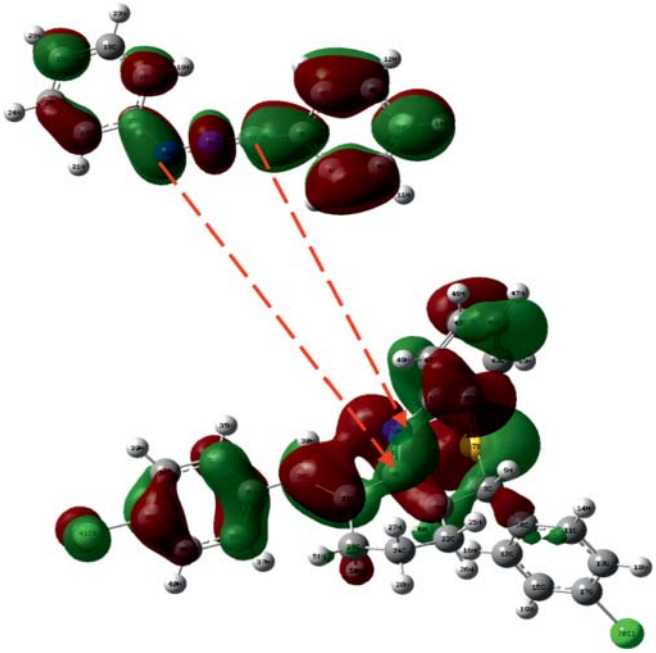

Fig. 4. Molecular orbital plot for the LUMO of compound **6** (above) and HOMO of **3** (below) in the orientation to form compound **9**.

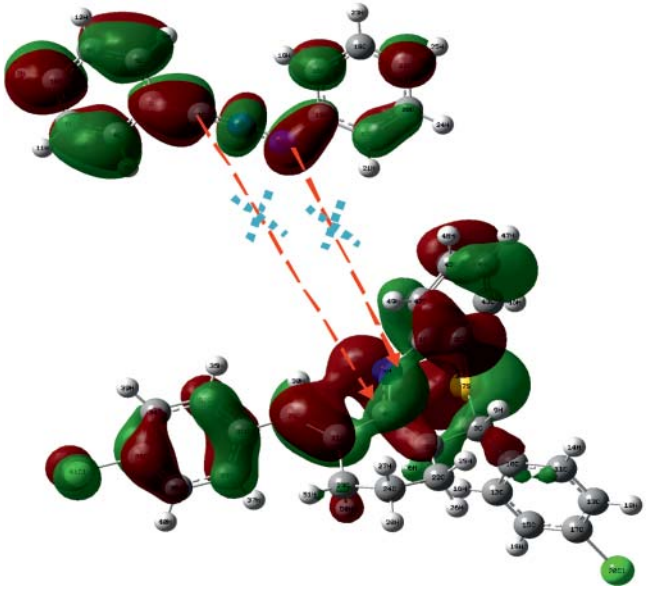

Fig. 5. Molecular orbital plot for the LUMO of compound **6** (above) and HOMO of **3** (below) in the orientation to form compound **10**.

postulated mechanism. We expected that the reaction proceed through the interaction of HOMO of one reactant with LUMO of the other as usually interpreted in cycloaddition reactions. An obvious pattern by which route the organic reaction will proceed is obtained by contrasting the signs of the molecular orbital (MO) lobes at the reaction sites. Similar signs of the lobes indicate constructive interference (bonding

Scheme 3.

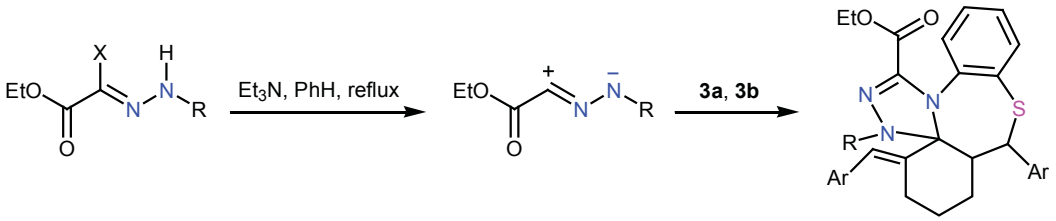

11 **12** **13a–13e**

13, Ar = 4-ClC_6H_4 (**a**–**c**), 4-FC_6H_4 (**d**, **e**); R = 4-MeC_6H_4 (**a**, **d**), 4-ClC_6H_4 (**b**), 4-$O_2NC_6H_4$ (**c**, **e**).

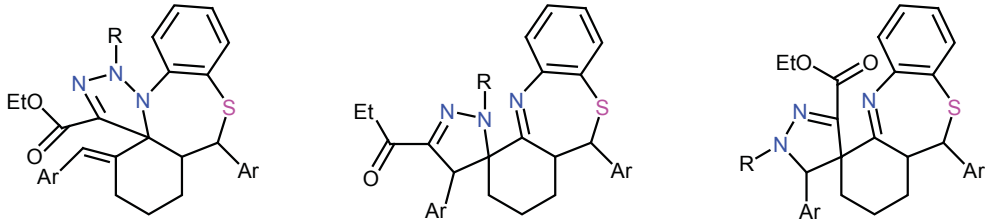

14 **15** **16**

overlap), while different sings indicate destructive interference (anti-bonding overlap). Figures 2–5 show the LUMO of **6** and HOMO of **3** in different orientations to each other to form compound **7**–**10**. It is clear that Figs. 2 and 4 correspond to the constructive reaction, whereas it is destructive in Figs. 3 and 5. Thus, the formation of **7** and **9** is possible, and the formation of **8** and **10** is not. Joint consideration of the total energies and molecular orbital interactions led us to conclude that the only possible pathway of the reaction between **3** and **6** is to produce compound **7**.

The reactions of **3a** and **3b** with *C*-ethoxycarbonyl-*N*-aryl nitrile imines **12** generated in situ from the corresponding hydrazonoyl chlorides **11** in refluxing benzene in the presence of triethylamine also yielded only one product in each case (compounds **13a**–**13e**; Scheme 3). The structure of the isolated compounds was determined on the basis of their IR, ^{1}H NMR, and mass spectra and elemental analyses (see Experimental). The other possible isomeric structures, **14**–**16** (Scheme 3) were thus discarded. For example, the ^{1}H NMR spectra of the products lacked dihydropyra-

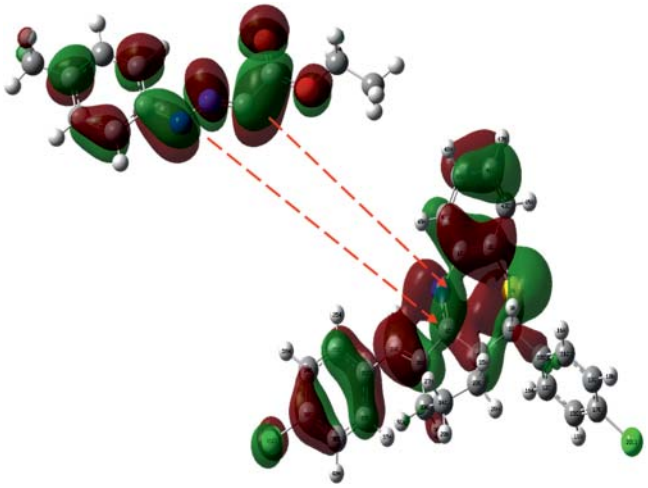

Fig. 6. Molecular orbital plot for the LUMO+1 of compound **12** (above) and HOMO of **3** (below) in the orientation to form compound **13**.

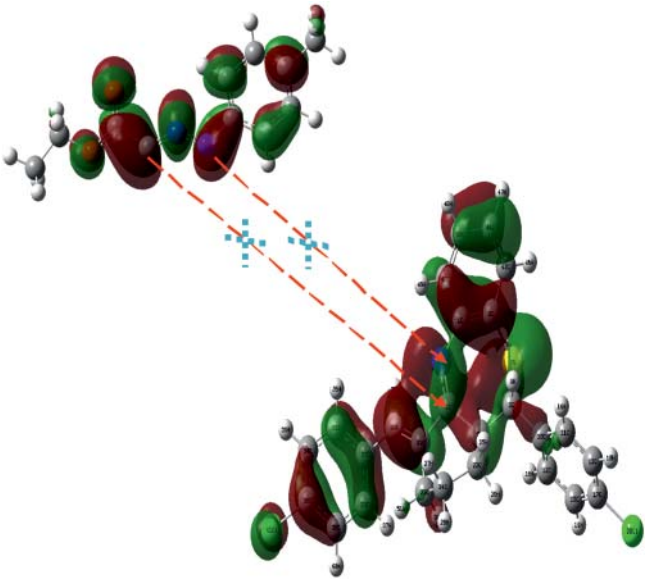

Fig. 7. Molecular orbital plot for the LUMO+1 of compound **12** (above) and HOMO of **3** (below) in the orientation to form compound **14**.

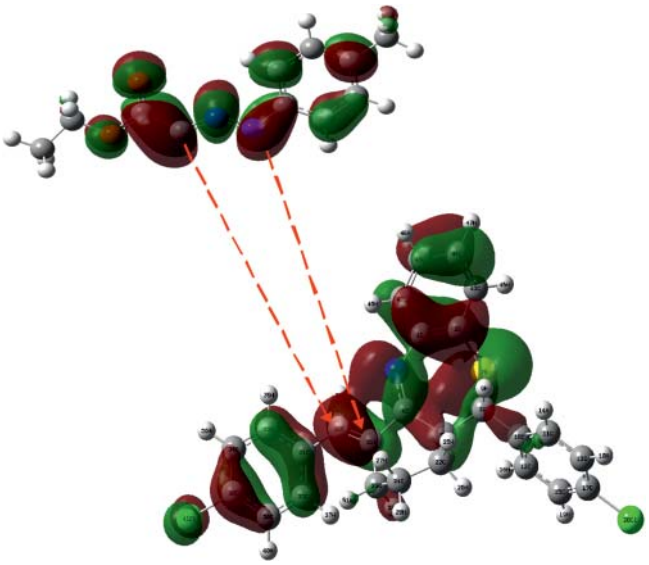

Fig. 8. Molecular orbital plot for the LUMO+1 of compound **12** (above) and HOMO of **3** (below) in the orientation to form compound **15**.

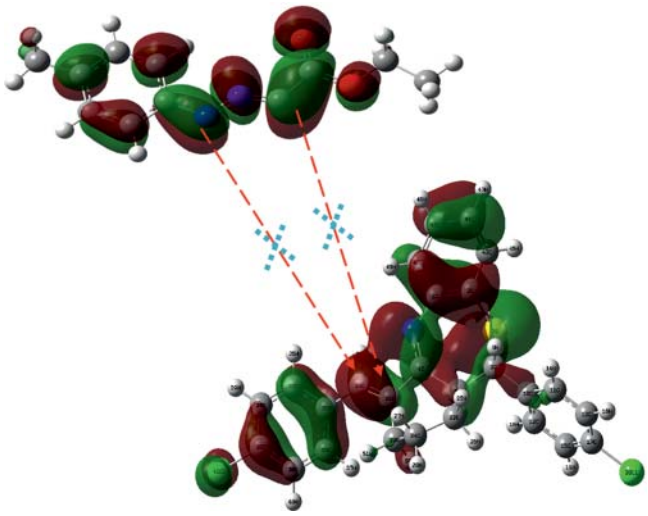

Fig. 9. Molecular orbital plot for the LUMO+1 of compound **12** (above) and HOMO of **3** (below) in the orientation to form compound **16**.

zole 4-H proton signal found in the spectra of **7**. These findings indicated that the products obtained in the reaction of **3** with **12** resulted from 1,3-dipolar cycloaddition of the latter to the endocyclic C=N double bond rather than to the exocyclic C=C bond.

A similar treatment can be applied for the reaction of **3** with **12** to yield one of compounds **13**–**16**. As followed from the total energy calculations, compounds **13** and **14** are more stable than **15** and **16** by more than 30 kcal/mol. The molecular orbital simulation showed that the LUMO of **12** has no π* character, so that the first π*-molecular orbital is LUMO+1. Figures 6–9 show the LUMO+1 of **12** and HOMO of **3** in the orientations required to form structures **13**–**16**. The reaction is constructive in the cases corresponding to Figs. 6 and 8 and is destructive in the cases depicted in Figs. 7 and 9. These MO plots indicate the possibility of formation of **13** and **15**. Likewise, a combination of the total energy and molecular orbital considerations suggested only one possibility, i.e., the formation of only compound **13**.

To explore the significance of the newly synthesized compounds, the in vitro antitumor activity of dibenzothiazepine derivatives **3**, **7**, and **13** was tested at the Regional Center for Mycology and Biotechnology (Al-Azhar University, Cairo, Egypt) against MCF-7 breast cancer cell line; doxorubicin (IC_{50} = 0.426 μg·mL^{-1}) was used as reference drug. The results are collected in Table 2. Compounds **3b**, **13a**, **13b**, and **13c** showed a promising pharmacological activity (IC_{50} = 2.7, 2.9, 6.2, and 13.5 μg/mL, respectively), while the activity of the other tested compounds was only moderate. It is important that the conversion of compound **3a** (IC_{50} = 24.8 μg/mL) into triazole derivatives **13a**–**13c** enhanced the antitumor activity.

Table 3 shows the results of theoretical toxicity predictions for dibenzothiazepine series **3**, **7**, and **13** using the Osiris program; it was found that the toxicity of all these compounds is lower than that of doxorubicin (DOX). It should also be noted that dibenzothiazepine **7d** can be used as antibiotic with some pharmacomodulation (DS = 1.85). It follows from the data in Table 3 that the tested structures are nonmutagenic. With regard to irritant and reproductive effects, all dibenzothiazepine compounds **3**, **7**, and **13** are at low risk compared to the standard medicine used. The hydrophilicity character of each derivative was expressed in terms of *c*Log*P* value. It has been shown that absorption or permeability is significantly affected by hydrophilicity (*c*Log*P* value). When the *c*Log*P* value is greater than five, the permeability or absorption decreases. On this basis, most dibenzothiazepine derivatives have *c*Log*P* values outside accepted range, but another critical parameter must be considered. This is related to the geometric structure of the pharmacophore site (Fig. 10) which is flexible in all benzothiazepine derivatives. The absorption, distribution properties, and bio-efficiency proved to be dependent on the geometrical parameters and solubility in water.

Further, drug-likeness (DL) of **3**, **7**, and **13** is not in the comparable zone with the standard drug used (Table 3). We have estimated DS (the overall drug

Table 2. Cytotoxicity of compounds **3a**, **3b**, **7a**–**7c**, **7e**, **7g**, **7i**, and **13a**–**13c** against MCF-7 cancer cell line

Compd. no.	IC_{50} (μg/mL)	Compd. no.	IC_{50} (μg/mL)
3a	24.8	**7g**	>50
3b	2.70	**7i**	46.2
7a	35.1	**13a**	6.20
7b	28.7	**13b**	2.90
7c	26.4	**13c**	13.5
7e	37.2	Doxorubicin	0.426

score) for dibenzothiazepine derivatives **3**, **7**, and **13** and compared it with that of the standard drug (doxorubicin). The drug score is an integral parameter comprising drug-likeness, *c*Log*S*, *c*Log*P*, toxicity risks, and molecular weight in one handy value that may be applied to judge the overall ability of tested compound to qualify for a drug. The newly synthesized compounds showed low to moderate DS values in comparison to DOX (Tables 3, 4).

CONCLUSION

We succeeded in synthesizing a new series of spiro-1,2,4-triazole derivatives containing a hexahydrodibenzo[*b*,*e*][1,4]thiazepine moiety, starting from commercially available compounds. The antitumor activity of these molecules was evaluated against breast cancer cell line (MCF-7) using doxorubicin as reference. Compound **13b** showed higher cytotoxicity than all other tested compounds; however, its biological activity remains modest (IC_{50} = 2.90 μg/mL) in comparison to doxorubicin (IC_{50} = 0.426 μg/mL). The results of POM analysis of the relative cytotoxicity of these new derivatives in comparison to doxorubicin have been reported. It seems that compounds of the **7a**–**7i** series possess an important antiparazite/antifungal and antiviral N,N-pharmacophore site which deserves a separate antiviral/antiparasite screening. Our previous experience with similar spiro systems suggests that a subtle change in the pharmacophore can give rise to antitubercular, antitumor, antitrypanosomal, and/or anti-HIV activities.

EXPERIMENTAL

Melting points were determined on a Stuart SMP3 melting point apparatus using 0.5-mm (o.d.) glass capillaries. The IR spectra (4000 to 200 cm^{-1}) were recorded on a Perkin Elmer 1430 spectrophotometer from samples prepared as KBr discs. The NMR spectra

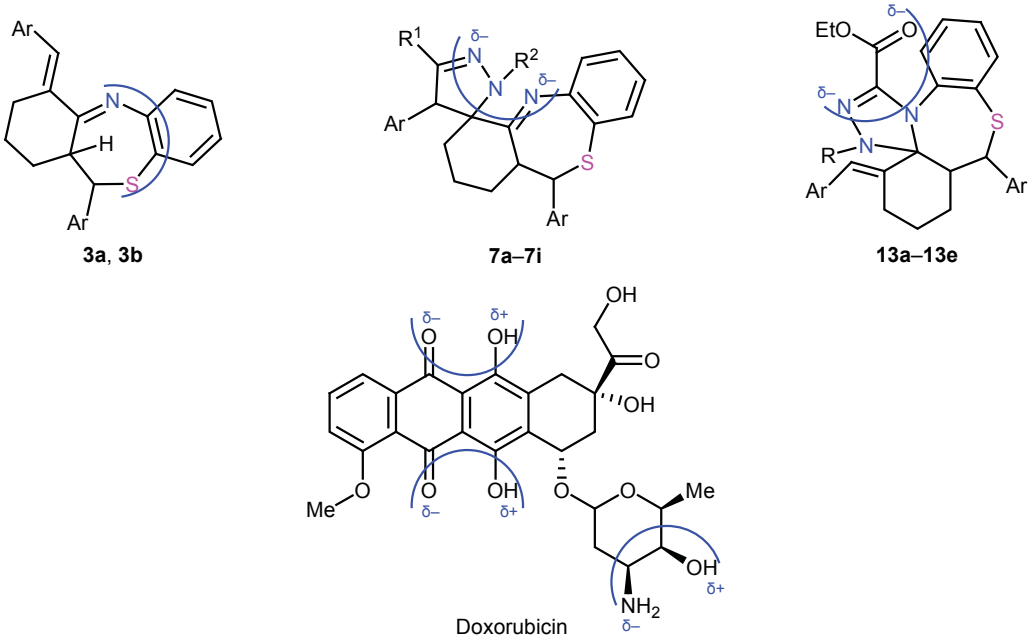

Fig. 10. Identification of pharmacophore sites on the basis of POM theory [19–34].

Table 3. Osiris calculations of toxicity risks[a] of dibenzothiazepine derivatives **3**, **7**, and **13**

Compd. no.	MW	Toxicity Risks[b]				Osiris calculations[c]			
		MUT	TUM	IRRIT	REP	*c*Log*P*	*S*	DL	DS
3a	449	+++	+++	+++	+++	7.55	–7.80	1.71	0.22
3b	417	+++	+++	+++	+++	6.54	–6.95	–0.04	0.21
7a	644	+++	+++	+++	+++	10.5	–10.3	1.42	0.13
7b	679	+++	+++	+++	+++	11.1	–11.1	1.42	0.12
7c	689	+++	+++	+++	+++	10.5	–10.9	1.02	0.12
7d	695	+++	+++	+++	+++	10.1	–10.8	1.85	0.13
7e	611	+++	+++	+++	+++	9.44	–9.5	0.07	0.12
7f	646	+++	+++	+++	+++	10.1	–10.2	0.08	0.11
7g	656	+++	+++	+++	+++	9.53	–9.94	–0.35	0.12
7h	662	+++	+++	+++	+++	9.40	–9.95	0.47	0.11
7i	646	+++	+++	+++	+++	8.72	–9.62	–0.35	0.10
13a	654	+++	+++	+++	+++	9.43	–9.61	–1.35	0.09
13b	675	+++	+++	+++	+++	9.69	–10.01	–1.35	0.08
13c	685	+++	+++	+++	+++	9.17	–9.72	–1.51	0.09
13d	621	+++	+++	+++	+++	8.41	–8.76	–2.76	0.08
13e	652	+++	+++	+++	+++	8.16	–8.88	–2.92	0.08
DOX[d]	543	+++	+++	---	+++	0.17	–4.51	7.19	0.33

[a] Higly toxic (---), slightly toxic: (+), nontoxic (+++).
[b] MUT: mutagenic; TUM: tumorigenic, IRRIT: irritant, REP: reproductive effects.
[c] S: solubility, DL: drug likeness, DS: drug score.
[d] Doxorubicin.

Table 4. Molinspiration calculations of compounds **3**, **7**, and **13**

Compd. no.	Molinspiration calculations[a]				Drug-likeness[b]					
	TPSA	NONH	NV	VOL	GPCRL	ICM	KI	NRL	PI	EI
3a	12	0	1	385	–0.27	–0.19	–0.56	–0.29	–0.28	–0.20
3b	12	0	1	368	–0.26	–0.20	–0.52	–0.26	–0.26	–0.18
7a	28	3	2	559	–0.39	–0.93	–0.99	–0.63	–0.34	–0.60
7b	28	3	2	573	–0.45	–1.05	–1.08	–0.74	–0.35	–0.70
7c	74	0	2	582	–0.70	–1.36	–1.39	–1.04	–0.55	–0.97
7d	74	0	2	573	–0.72	–1.32	–1.31	–1.02	–0.56	–0.91
7e	28	0	2	542	–0.38	–0.94	–0.96	–0.61	–0.33	–0.61
7f	28	0	2	555	–0.45	–1.06	–1.07	–0.73	–0.39	–0.71
7g	28	0	2	555	–0.45	–1.06	–1.07	–0.73	–0.39	–0.71
7h	78	0	2	556	–0.72	–1.33	–1.29	–1.00	–0.55	–0.90
7i	87	0	2	545	–0.72	–1.32	–1.34	–0.99	–0.62	–0.92
13a	45	0	2	566	–0.42	–1.01	–0.98	–0.64	–0.36	–0.64
13b	45	0	2	563	–0.40	–0.97	–0.96	–0.62	–0.33	–0.61
13c	91	0	2	572	–0.62	–1.26	–1.24	–0.89	–0.48	–0.85
13d	45	0	2	548	–0.42	–1.02	–0.95	–0.61	–0.35	–0.63
13e	91	0	2	555	–0.62	–1.26	–1.21	–0.87	–0.47	–0.84
DOX	206	7	3	459	0.20	–0.20	–0.07	0.32	0.67	0.66

[a] TPSA: total molecular polar surface area; NONH: number of OH···N or O···NH interaction, NV: number of violations of Lipinski's rule of five; VOL: volume.
[b] GPCRL: GPCR ligand; ICM: ion channel modulator; KI: kinase inhibitor; NRL: nuclear receptor ligand; PI: protease inhibitor; EI: enzyme inhibitor.

were acquired on a Bruker Avance 400 instrument at 400 MHz for ^{1}H in DMSO-d_6 solutions, using the residual solvent signal as reference. The mass spectra (electron impact, 70 eV) were obtained on a Finnigan-MAT 8222 instrument at the Microanalytical Center (Cairo University). Elemental analyzes were carried out on a Vario-LIII Elementar CHNS analyzer (Germany). Initial compounds **1a**, and **1b** and hydrazonoyl chlorides **5** and **11** were prepared as reported previously [35–37].

Compounds 3a and 3b (*general procedure*). A mixture of 1.7 g (5 mmol) of 2,6-bis(4-chlorobenzylidene)cyclohexan-1-one (**1a**) or 1.6 g (5 mmol) of 2,6-bis(4-fluorobenzylidene)cyclohexan-1-one (**1b**), 0.65 g (5 mmol) of 2-aminobenzenethiol (**2**), and 3 mL of acetic acid in 30 mL of ethanol was refluxed for 5 h. The solvent was evaporated under reduced pressure, and the product was filtered off and recrystallized from ethanol.

4-(4-Chlorobenzylidene)-11-(4-chlorophenyl)-1,2,3,4,11,11a-hexahydrodibenzo[*b*,*e*][1,4]thiazepine (3a). Yield 1.6 g (70%), yellow crystals, mp 180–182°C. IR spectrum, ν, cm^{-1}: 3055, 2927, 2859, 1553, 1483, 1443, 1093. ^{1}H NMR spectrum, δ, ppm: 1.11–1.80 m and 2.53–3.17 m (7H, CH_2, CH), 5.05 d (J = 12.6 Hz , 1H, CH), 7.15 – 7.58 m (13H, Ar-H, =CH); ^{13}C NMR spectrum, δ_C, ppm: 23.12, 27.0, 27.9, 39.1, 57.21, 119.6, 125.8, 126.9, 127.5, 128.2, 129.0, 130.1, 130.4, 131.5 131.9, 133.2, 134.4, 135.3, 136.3, 150.2, 152.1, 165.8. Mass spectrum, m/z (I_{rel}, %): 452 (1) $[M + 2]^+$, 451 (6) $[M + 1]^+$, 450 (6) $[M]^+$, 353 (35), 338 (100), 323 (24), 311 (18), 308 (19), 126 (24), 90 (19), 76 (24), 63 (28), 50 (24) Found, %: C 69.21; H 4.56; N 3.02. $C_{26}H_{21}Cl_2NS$. Calculated, %: C 69.33; H 4.70; N 3.11. M 450.42.

4-(4-Fluorobenzylidene)-11-(4-fluorophenyl)-1,2,3,4,11,11a-hexahydrodibenzo[*b*,*e*][1,4]thiazepine (3b). Yield 1.7 g (80%), yellow fluorescing crystals, mp 174–176°C. IR spectrum, ν, cm^{-1}: 3052, 2935, 2841, 1567, 1482, 1440, 1093. ^{1}H NMR spectrum, δ, ppm: 1.06–1.85 m and 3.00–3.14 m (7H, CH_2, CH), 5.05 d (1H, J = 12.6 Hz, CH), 7.10–7.31 m and 7.45–7.61 m (12H, H_{arom}, =CH), 7.38 s (1H, =CH). ^{13}C NMR spectrum, δ_C, ppm: 22.70, 27.10, 29.37, 37.12, 57.54, 120.27, 123.93, 125.90, 128.27, 128.36, 129.28, 131.54, 134.21, 135.36, 135.94, 136.65, 137.10, 140.54, 147.15, 149.33, 150.11, 163.12. Mass spectrum, m/z (I_{rel}, %): 419 (4) $[M + 2]^+$, 418 (10) $[M + 1]^+$, 417 (32) $[M]^+$, 308 (10), 280 (5), 270 (12), 268 (100), 254 (12), 162 (5), 160 (5), 149 (6), 146 (10), 136 (8), 133 (28), 109 (44), 107 (6), 83 (7), 69 (7). Found, %: C 74.57; H 5.16; N 3.19. $C_{26}H_{21}F_2NS$. Calculated, %: C 74.79; H 5.07; N 3.35. M 417.51.

Compounds 7a–7i and 13a–13e (*general procedure*). Triethylamine (0.28 mL, 2 mmol), was added to a mixture of equimolar amounts of compound **3a** (0.9 g, 2 mmol) or **3b** (0.84 g, 2 mmol) and the corresponding hydrazonoyl chloride **5** (in the synthesis of **7a**–**7i**) or **11** (in the synthesis of **13a**–**13e**) (2 mmol) in dry benzene (30 mL), and the mixture was refluxed for 20 h. The solvent was evaporated, the liquid residue was triturated with methanol, and the solid product was collected by filtration under vacuum and crystallized from dioxane.

4′,11-Bis(4-chlorophenyl)-2′,5′-diphenyl-2,2′,3,4′,11,11a-hexahydro-1*H*-spiro[dibenzo[*b*,*e*]-[1,4]thiazepine-4,3′-pyrazole] (7a). Yield 0.64 g (50%), greenish brown solid, mp 220–222°C. IR spectrum, ν, cm^{-1}: 3048, 2928, 2866, 1625, 1589, 1487, 1451, 1371, 1285, 1091. ^{1}H NMR spectrum, δ, ppm: 1.06–1.70 m and 3.38–4.40 m (7H, CH_2, CH), 5.45 d (1H, J = 12.6 Hz, C–H), 5.50 s (1H, 4′-H), 6.58–7.71 m (22H, H_{arom}). ^{13}C NMR spectrum, δ_C, ppm: 21.0, 26.27, 28.2, 36.7, 57.6, 80.2, 117.8, 118.2, 121.1, 122.0, 124.3, 125.9, 127.1, 127.6, 128.7, 128.9, 129.1, 129.3, 130.2, 130.4, 131.8, 133.5, 134.1, 134.5, 136.4, 137.5, 140.7, 145.4, 152.6, 154.7, 160.2. Mass spectrum, m/z (I_{rel}, %): 646 (11) $[M + 2]^+$, 645 (23) $[M + 1]^+$, 644 (23) $[M]^+$, 642 (25), 370 (18), 359 (35), 357 (100), 344 (25), 342 (20), 321 (18), 286 (24), 272 (16), 268 (22), 204 (19), 162 (48), 136 (16), 128 (25), 125 (40), 118 (15), 115 (15), 104 (15), 96 (23), 91 (17), 77 (50), 65 (17). Found, %: C 72.48; H 4.62; N 6.41%. $C_{39}H_{31}Cl_2N_3S$. Calculated, %: C 72.66; H 4.85; N 6.52. M 644.66.

4′,5′,11-Tris(4-chlorophenyl)-2′-phenyl-2,2′,3,4′,11,11a-hexahydro-1*H*-spiro[dibenzo[*b*,*e*]-[1,4]thiazepine-4,3′-pyrazole] (7b). Yield 0.68 g (50%), brown solid, mp 210–212°C. IR spectrum, ν, cm^{-1}: 3053, 2928, 2860, 1588, 1485, 1286, 1257, 1093. ^{1}H NMR spectrum, δ, ppm: 1.11–2.36 m and 2.99–3.16 m (7H, CH_2, CH), 5.06 d (1H, J = 12.6 Hz, CH), 5.47 s (1H, 4′-H), 6.60–8.27 m (21H, H_{arom}). Mass spectrum, m/z (I_{rel}, %): 680 (10) $[M + 2]^+$, 679 (13) $[M + 1]^+$, 678 (24) $[M]^+$, 676 (24), 575 (25), 573 (50), 571 (47), 393 (45), 391 (77), 379 (19), 377 (32), 340 (15), 338 (23), 302 (17), 286 (40), 284 (52), 274 (17), 272 (33), 204 (19), 162 (39), 149 (19), 138 (16), 136 (29), 127 (17), 125 (33), 115 (31), 108 (17), 102 (17), 91 (37), 89 (21), 77 (100), 64 (23), 51 (19). Found, %: C 69.05; H 4.34; N 6.36. $C_{39}H_{30}Cl_3N_3S$. Calculated, %: C 68.98; H 4.45; N 6.19. M 679.10.

4′,11-Bis(4-chlorophenyl)-2′-(4-nitrophenyl)-5′-phenyl-2,2′,3,4′,11,11a-hexahydro-1*H*-spiro[dibenzo[*b*,*e*][1,4]thiazepine-4,3′-pyrazole] (7c). Yield 0.87 g (63%), red crystals, mp 226–228°C (from EtOH). IR spectrum, ν, cm^{-1}: 2923, 2855, 1588, 1489, 1455, 1296, 1102. ^1H NMR spectrum, δ, ppm: 0.77–1.78 m and 2.99–3.32 m (7H, CH_2, CH), 5.04 d (1H, J = 12.6 Hz , CH), 5.66 s (1H, 4′-H), 6.57–8.19 m (21H, H_{arom}). Mass spectrum, *m*/*z* (I_{rel}, %): 690 (2) $[M + 1]^+$, 689 (2) $[M]^+$, 540 (75), 537 (100), 536 (34), 380 (20), 372 (26), 284 (26), 272 (19), 204 (16), 151 (19), 149 (16), 136 (25), 129 (23), 127 (25), 125 (37), 115 (48), 109 (16), 105 (16), 103 (21), 91 (19), 89 (35), 77 (46), 64 (22), 62 (21), 51 (21). Found, %: C 68.12; H 4.49; N 8.26. $C_{39}H_{30}Cl_2N_4O_2S$. Calculated, %: C 67.92; H 4.38; N 8.12. *M* 689.65.

4′,11-Bis(4-chlorophenyl)-2′-(4-nitrophenyl)-5′-(thiophen-2-yl)-2,2′,3,4′,11,11a-hexahydro-1*H*-spiro[dibenzo[*b*,*e*][1,4]thiazepine-4,3′-pyrazole] (7d). Yield 0.79 g (57%), red crystals, mp 248–250°C (from EtOH). IR spectrum, ν, cm^{-1}: 3061, 2923, 2858, 1586, 1490, 1377, 1294. ^1H NMR spectrum, δ, ppm: 1.03–1.90 m and 2.51–3.10 m (7H, CH_2, CH), 5.35 d (1H, J = 12.6 Hz, CH), 5.58 s (1H, 4′-H), 6.46–8.19 m (19H, H_{arom}). Mass spectrum, *m*/*z* (I_{rel}, %): 697 (5) $[M + 2]^+$, 696 (3) $[M + 1]^+$, 695 (20) $[M]^+$, 663 (23), 545 (60), 544 (50), 543 (53), 542 (83), 272 (33), 139 (30), 126 (23), 115 (37), 103 (47), 85 (37), 84 (33), 77 (43). Found, %: C 63.95; H 4.31; N 7.98. $C_{37}H_{28}Cl_2N_4O_2S_2$. Calculated, %: C 63.88; H 4.06; N 8.05. *M* 695.68.

4′,11-Bis(4-fluorophenyl)-2′,5′-diphenyl-2,2′,3,4′,11,11a-hexahydro-1*H*-spiro[dibenzo[*b*,*e*]-[1,4]thiazepine-4,3′-pyrazole] (7e). Yield 0.59 g (48%), white crystals, mp 214–216°C (from EtOH). IR spectrum, ν, cm^{-1}: 3049, 2924, 2864, 1595, 1499, 1452, 1373, 1289. ^1H NMR spectrum, δ, ppm: 1.12–2.40 m and 3.20–3.25 m (7H, CH_2, CH), 5.45 d (1H, J = 12.6 Hz, CH), 5.52 s (1H, 4′-H), 6.59 d (4H, J = 8 Hz, H_{arom}), 6.89–7.41 m (14H, H_{arom}), 7.69 d (4H, J = 8 Hz, H_{arom}). Mass spectrum, *m*/*z* (I_{rel}, %): 613 (2) $[M + 2]^+$, 612 (9) $[M + 1]^+$, 611 (17) $[M]^+$, 506 (100), 504 (24), 356 (14), 341 (71), 327 (31), 306 (16), 270 (17), 268 (34), 267 (18), 256 (13), 251 (16), 224 (13), 162 (11), 147 (10), 136 (16), 133 (21), 115 (13), 109 (51), 107 (14), 104 (16), 91 (24), 77 (69), 65 (13), 51 (16). Found, %: C 76.72; H 5.35; N 6.59. $C_{39}H_{31}F_2N_3S$. Calculated, %: C 76.57; H 5.11; N 6.87. *M* 611.75.

5′-(4-Chlorophenyl)-4′,11-bis(4-fluorophenyl)-2′-phenyl-2,2′,3,4′,11,11a-hexahydro-1*H*-spiro[dibenzo[*b*,*e*][1,4]thiazepine-4,3′-pyrazole] (7f). Yield 0.52 g (40%), yellow crystals, mp 60–62°C (from EtOH). IR spectrum, ν, cm^{-1}: 3058, 2921, 2852, 1596, 1550, 1503, 1404, 1369, 1305. ^1H NMR spectrum, δ, ppm: 0.74–3.15 m (7H, CH_2, CH), 5.50 d (1H, J = 13 Hz, CH), 5.40 s (1H, 4′-H), 6.93–7.65 m (21H, H_{arom}). Mass spectrum, *m*/*z* (I_{rel}, %): 647 (8) $[M + 2]^+$, 646 (11) $[M + 1]^+$, 645 (21) $[M]^+$, 643 (17), 377 (37), 375 (86), 361 (16), 270 (25), 268 (100), 256 (17), 162 (25), 133 (18), 109 (39), 107 (16), 77 (38). Found, %: C 72.58; H 4.39; N 6.58. $C_{39}H_{30}ClF_2N_3S$. Calculated, %: C 72.49; H 4.68; N 6.50. *M* 646.19.

4′,11-Bis(4-fluorophenyl)-2′-(4-nitrophenyl)-5′-phenyl-2,2′,3,4′,11,11a-hexahydro-1*H*-spiro[dibenzo[*b*,*e*][1,4]thiazepine-4,3′-pyrazole] (7g). Yield 0.83 g (63%), orange crystals, mp 254–256°C. IR spectrum, ν, cm^{-1}: 3063, 2933, 1590, 1500, 1388, 1306. ^1H NMR spectrum, δ, ppm: 1.14–2.43 m and 2.75–3.27 m (7H, CH_2, CH), 5.46 d (1H, J = 13 Hz, CH), 5.67 s (1H, 4′-H), 6.50–8.32 m (21H, H_{arom}). Mass spectrum, *m*/*z* (I_{rel}, %): 656 (13), $[M]^+$, 506 (100), 504 (18), 472 (21), 396 (22), 394 (13), 372 (23), 364 (28), 256 (30), 327 (13), 325 (12), 312 (10), 270 (21), 268 (43), 257 (14), 256 (23), 253 (12), 250 (10), 236 (12), 222 (15), 207 (10), 197 (13), 185 (10), 183 (16), 177 (10), 168 (10), 165 (10), 151 (10), 146 (14), 135 (25), 133 (25), 121 (16), 110 (15), 108 (33), 105 (14), 103 (15), 101 (13), 95 (13), 91 (14), 89 (22), 82 (12), 78 (12), 76 (23), 74 (10), 65 (22), 63 (16), 51 (15). Found, %: C 71.52; H 4.84; N 8.24. $C_{39}H_{30}F_2N_4O_2S$. Calculated, %: C 71.32; H 4.60; N 8.53. *M* 656.74.

4′,11-Bis(4-fluorophenyl)-2′-(4-nitrophenyl)-5′-(thiophen-2-yl)-2,2′,3,4′,11,11a-hexahydro-1*H*-spiro[dibenzo[*b*,*e*][1,4]thiazepine-4,3′-pyrazole] (7h. Yield 0.68 g (51%), orange crystals, mp 218–220°C. IR spectrum, ν, cm^{-1}: 3444, 2934, 2869, 2589, 1502, 1448, 1377, 1294. ^1H NMR spectrum, δ, ppm: 1.12–2.80 m (7H, CH_2, CH), 4.91 s (1H, 4′-H), 5.38 d (1H, J = 13 Hz, CH), 6.47–8.28 m (19H, H_{arom}). Mass spectrum, *m*/*z* (I_{rel}, %): 664 (12) $[M + 2]^+$, 663 (4) $[M + 1]^+$, 662 (39) $[M]^+$, 567 (21), 472 (15), 440 (30), 364 (23), 309 (11), 241 (15), 122 (5), 95 (63), 83 (16), 76 (34). Found, %: C 67.25; H 4.39; N 8.18. $C_{37}H_{28}F_2N_4O_2S_2$. Calculated, %: C 67.05; H 4.26; N 8.45. *M* 662.77.

4′,11-Bis(4-fluorophenyl)-5′-(furan-2-yl)-2′-(4-nitrophenyl)-2,2′,3,4′,11,11a-hexahydro-1*H*-spiro-[dibenzo[*b*,*e*][1,4]thiazepine-4,3′-pyrazole] (7i). Yield 0.84 g (65%), red crystals, mp 250–252°C (from EtOH). IR spectrum, ν, cm^{-1}: 3070, 2923, 2858, 1590, 1502, 1453, 1371, 1323, 1302. ^1H NMR spectrum, δ, ppm: 1.03–3.44 m (7H, CH_2, CH), 5.34 d (1H, J = 13 Hz, CH), 5.49 s (1H, 4′-H), 6.51–8.19 m (19H,

H_{arom}). Mass spectrum, *m*/*z* (I_{rel}, %): 646 (10) $[M]^+$, 495 (100), 462 (17), 346 (20), 268 (26), 256 (21), 147 (15), 139 (15), 136 (13), 133 (20), 121 (14), 115 (22), 109 (44), 93 (17), 77 (17), 75 (16), 67 (15), 65 (22), 63 (19), 58 (15), 53 (13), 51 (24). Found, %: C 68.97; H 4.15; N 8.54. $C_{37}H_{28}F_2N_4O_3S$. Calculated, %: C 68.72; H 4.36; N 8.66. *M* 646.71.

Ethyl 4-(4-chlorobenzylidene)-8-(4-chlorophenyl)-3-(4-methylphenyl)-4,5,6,7,7a,8-hexahydro-3*H*-dibenzo[*b*,*e*][1,2,4]triazolo[4,3-*d*][1,4]thiazepine-1-carboxylate (13a). Yield 0.68 g (52%), yellow solid, mp 130–132°C. IR spectrum, ν, cm^{-1}: 3045, 2925, 2857, 1700 (C=O), 1575, 1480, 1376. ^1H NMR spectrum, δ, ppm: 0.83 t (3H, *J* = 7 Hz, CH_3), 1.09–1.80 m and 2.80–3.15 m (6H, CH_2), 2.39 s (3H, CH_3), 3.88 q (2H, *J* = 6 Hz, OCH_2), 4.70 m (1H, CH), 5.06 d (1H, *J* = 12 Hz, CH), 7.19–7.63 m (17H, H_{arom}, =CH). ^{13}C NMR spectrum, δ_C, ppm: 14.1, 19.4, 23.5, 28.1, 30.3, 40.7, 54.8, 62.2, 109.3, 115.8, 119.4, 120.6, 122.0, 124.3, 125.5, 126.6, 127.5, 128.2, 129.1, 129.9, 130.7, 131.6, 132.0, 133.2, 133.7, 137.6, 141.7, 142.5, 146.2, 155.4, 159.3. Mass spectrum, *m*/*z* (I_{rel}, %): 655 (27) $[M + 1]^+$, 654 (33) $[M]^+$, 630 (26), 601 (31), 597 (26), 592 (31), 590 (27), 554 (26), 532 (39), 523 (33), 521 (31), 513 (29), 509 (31), 507 (35), 506 (33), 502 (34), 499 (27), 489 (32), 486 (30), 460 (100), 451 (28), 443 (29), 404 (38), 397 (36), 386 (37), 377 (32), 367 (31), 365 (63), 363 (34), 336 (36), 332 (70), 298 (32), 284 (30), 256 (32), 245 (43), 240 (32), 201 (38), 194 (27), 179 (32), 130 (35), 100 (33), 80 (27), 72 (28). Found, %: C 67.75; H 5.14; N 6.53. $C_{37}H_{33}Cl_2N_3O_2S$. Calculated, %: C 67.88; H 5.08; N 6.42. *M* 654.65.

Ethyl 4-(4-chlorobenzylidene)-3,8-bis(4-chlorophenyl)-4,5,6,7,7a,8-hexahydro-3*H*-dibenzo[*b*,*e*][1,2,4]triazolo[4,3-*d*][1,4]thiazepine-1-carboxylate (13b). Yield 0.65 g (48%), pale yellow solid, mp 142–144°C. IR spectrum, ν, cm^{-1}: 3045, 2924, 2856, 1702 (C=O), 1582, 1514, 1482, 1445, 1375. ^1H NMR spectrum, δ, ppm: 0.82 t (3H, *J* = 7 Hz, CH_3), 1.10–1.72 m and 2.78–3.18 m (6H, CH_2), 3.90 q (2H, *J* = 7 Hz, OCH2), 4.70 d (1H, *J* = Hz, CH), 5.05 d (1H, *J* = 12.3 Hz, CH), 7.14–7.62 m (17H, H_{arom}, =CH). Mass spectrum, *m*/*z* (I_{rel}, %): 675 (15) $[M]^+$, 674 (19), 597 (18), 565 (18), 493 (18), 486 (19), 462 (44), 460 (52), 451 (24), 449 (30), 404 (23), 396 (24), 332 (21), 323 (22), 296 (25), 288 (27), 286 (42), 284 (100), 274 (25), 271 (22), 248 (26), 235 (25), 224 (22), 192 (22), 181 (21), 163 (27), 153 (28), 149 (33), 136 (22), 129 (25), 127 (49), 125 (73), 121 (29), 117 (27), 115 (79), 113 (23), 111 (21), 109 (43), 105 (22), 102 (25), 99 (21), 94 (32), 91 (25), 89 (44), 80 (95), 77 (38), 72 (25), 69 (41), 64 (92). Found, %: C 64.14; H 4.16; N 6.29. $C_{36}H_{30}Cl_3N_3O_2S$. Calculated, %: C 64.05; H 4.48; N 6.22. *M* 675.07.

Ethyl 4-(4-chlorobenzylidene)-8-(4-chlorophenyl)-3-(4-nitrophenyl)-4,5,6,7,7a,8-hexahydro-3*H*-dibenzo[*b*,*e*][1,2,4]triazolo[4,3-*d*][1,4]thiazepine-1-carboxylate (13c). Yield 0.96 g (70%), orange solid, mp 180–182°C. IR spectrum, ν, cm^{-1}: 3055, 2925, 2853, 1699 (C=O), 1593, 1513, 1480, 1444, 1377. ^1H NMR spectrum, δ, ppm: 0.81 t (3H, *J* = 7 Hz, CH_3), 1.14–1.95 m and 2.67–3.20 m (6H, CH_2), 3.92 q (2H, *J* = 7 Hz, OCH_2), 4.70 m (1H, CH), 5.05 d (1H, *J* = 11.4 Hz, CH), 7.17–7.63 m (17H, H_{arom}, =CH). Mass spectrum, *m*/*z* (I_{rel}, %): 686 (17) $[M + 1]^+$, 685 (25) $[M]^+$, 661 (21), 598 (28), 574 (24), 553 (21), 505 (22), 498 (24), 494 (22), 481 (20), 475 (25), 455 (22), 406 (26), 393 (21), 367 (23), 363 (21), 354 (26), 349 (26), 342 (22), 338 (32), 326 (30), 312 (25), 300 (21), 288 (21), 282 (24), 263 (22), 247 (22), 224 (21), 218 (20), 213 (23), 210 (24), 199 (22), 194 (33), 180 (22), 178 (23), 161 (25), 152 (22), 145 (21), 141 (24), 126 (31), 120 (23), 115 (38), 113 (23), 111 (28), 93 (34), 90 (28), 86 (93), 80 (100), 76 (38). Found, %: C 63.12; H 4.51; N 8.02. $C_{36}H_{30}Cl_2N_4O_4S$. Calculated, %: C 63.06; H 4.41; N 8.17. *M* 685.62.

Ethyl 4-(4-fluorobenzylidene)-8-(4-fluorophenyl)-3-(4-methylphenyl)-4,5,6,7,7a,8-hexahydro-3*H*-dibenzo[*b*,*e*][1,2,4]triazolo[4,3-*d*][1,4]thiazepine-1-carboxylate (13d). Yield 0.84 g (68%), yellow solid, mp 194–196°C. IR spectrum, ν, cm^{-1}: 3045, 2929, 2859, 1700 (C=O), 1596, 1508, 1472, 1448, 1377. ^1H NMR spectrum, δ, ppm: 0.82 t (3H, *J* = 7 Hz, CH_3), 1.07–2.34 m and 2.68–3.20 m (6H, CH_2), 2.36 s (3H, CH_3), 3.91 q (2H, *J* = 7 Hz, OCH_2), 4.65 m (1H, CH), 5.03 d (1H, *J* = 11.7 Hz, CH), 7.03–7.61 m (17H, H_{arom}, =CH). Mass spectrum, *m*/*z* (I_{rel}, %): 622 (52) $[M + 1]^+$, 621 (51) $[M]^+$, 617 (45), 580 (81), 563 (45), 553 (48), 538 (54), 519 (61), 502 (68), 477 (42), 473 (45), 463 (50), 457 (46), 450 (45), 441 (65), 432 (46), 421 (51), 414 (45), 410 (63), 393 (53), 386 (45), 382 (47), 373 (62), 371 (48), 364 (100), 355 (57), 341 (53), 334 (88), 330 (63), 323 (63), 310 (86), 293 (62), 290 (47), 246 (64), 240 (75), 216 (51), 187 (48), 167 (42), 152 (42), 97 (64), 81 (55), 79 (58). Found, %: C 71.41; H 5.39; N 6.69. $C_{37}H_{33}F_2N_3O_2S$. Calculated, %: C 71.48; H 5.35; N 6.76. *M* 621.74.

Ethyl 4-(4-fluorobenzylidene)-8-(4-fluorophenyl)-3-(4-nitrophenyl)-4,5,6,7,7a,8-hexahydro-3*H*-dibenzo[*b*,*e*][1,2,4]triazolo[4,3-*d*][1,4]thiazepine-1-carboxylate (13e). Yield 0.91 g (70%), brown solid, mp 178–180°C. IR spectrum, ν, cm^{-1}: 3038, 2922,

2852, 1696 (C=O), 1598, 1505, 1474, 1441, 1373. ^{1}H NMR spectrum, δ, ppm: 0.82 t (3H, J = 7 Hz, CH_3), 1.15–1.90 m and 2.77–3.08 m (6H, CH_2), 3.89 q (2H, J = 7 Hz, OCH_2), 4.69 m (1H, CH), 5.04 d (1H, J = 11.4 Hz, CH), 7.13–7.63 m (17H, H_{arom}, =CH). Mass spectrum, m/z (I_{rel}, %): 655 (54) $[M + 3]^+$, 654 (47) $[M + 2]^+$, 653 (57) $[M + 1]^+$, 652 (19) $[M]^+$, 642 (51), 639 (45), 626 (55), 617 (56), 598 (45), 594 (70), 591 (43), 572 (46), 570 (57), 567 (46), 556 (56), 554 (56), 547 (54), 543 (43), 530 (62), 528 (46), 515 (47), 510 (50), 508 (41), 499 (66), 460 (65), 455 (58), 449 956), 442 (56), 400 (55), 397 (64), 382 (64), 360 (55), 337 (58), 330 (77), 319 (54), 306 (79), 300 (61), 263 (56), 239 (58), 229 (56), 218 (65), 201 (64), 199 (66), 190 (68), 176 (60), 174 (54), 170 (68), 166 (62), 154 (52), 148 (76), 145 (75), 132 (77), 106 (100), 102 (58). Found, %: C 66.19; H 4.59; N 8.52. $C_{36}H_{30}F_2N_4O_4S$. Calculated, %: C 66.24; H 4.63; N 8.58. M 652.71.

Quantum chemical calculations. Hybrid density functional theory B3LYP method [38–43] was utilized to calculate the molecular geometry of all newly synthesized dibenzothiazepine derivatives. All calculations were performed using Gaussian 09W software package [44]. The calculated structures were visualized using GaussView version 5.0.9 [45].

Anticancer activity. Eleven dibenzothiazepine derivatives **3a**, **3b**, **7a**–**7c**, **7e**, **7g**, **7i**, and **13a**–**13c** were tested against MCF-7 human breast cancer cell line by the known MTT [3-(4,5-dimethyl-1,3-thiazol-2-yl)-2,5-diphenyltetrazolium bromide] assay, and the results were compared with the data for doxorubicin used as reference drug. The IC_{50} values were determined from the dose–response curve plotted on the basis of the MTT assay data. The cytotoxicity was expressed as mean IC_{50} value for three independent runs (Table 2). The procedure was identical to that published by Vijayan et al. [46] using Crystal Violet dye (1%). The cells were siphoned into a 96-well plate to a concentration of 1×10^4 cells per well (100 μL). The microplates were incubated at 37°C for 48 h in a humidified incubator (5% CO_2). Three wells were used for each concentration value. Control wells contained only DMSO without any test compound. After incubation of cells for 24 h at 37°C, different concentrations of test samples (50, 25, 12.5, 6.25, 3.125, and 1.56 μg) were added, the incubation was continued for 48 h, and a solution of Crystal Violet was added to each well for at least 30 min. Excess dye was removed using tap water, 30% acetic acid (30%) was then added to each well, the content of the wells was thoroughly mixed, and the absorbance at λ 490 nm was measured using a microplate reader. All results were corrected for background absorption detected in the wells without adding a stain. All experiments were conducted in triplicate. The results are collected in Table 2.

CONFLICT OF INTEREST

The authors declare that they have no conflict of interest.

REFERENCES

1. Shawali, A.S., *Curr. Org. Chem*., 2014, vol. 18, p. 598. https://doi.org/10.2174/1385272819666140201002900
2. Papdopoulos, S. and Stephanidou, J.S., *J. Heterocycl. Chem*., 1987, vol. 24, p. 309. https://doi.org/10.1002/jhet.5570240203
3. Baba, N. and Soufiaoui, M., *Tetrahedron Lett*., 1990, vol. 31, p. 1709. https://doi.org/10.1016/S0040-4039(00)88860-7
4. Liu, B., Li, X-F., Liu, H-C., and Yu, X.-Y., *Tetrahedron Lett*., 2013, vol. 54, p. 6952. https://doi.org/10.1016/j.tetlet.2013.10.062
5. Abdel Hafez, N.A., Hassaneen, H.M.E., Farghaly, T.A., Riyadh, S., and Alzahaby, H., *Mini-Rev. Med. Chem*., 2018, vol. 18, p. 631. https://doi.org/10.2174/1389557517666170912170027
6. Shneine, J.K. and Alaraji, Y.H., *Int. J. Sci. Res*., 2016, vol. 5, no. 3, p. 1411. https://www.ijsr.net/archive/v5i3/NOV161902.pdf
7. Capozzi, G., Chimirri, A., Grasso, S., Romeo, G., and Zappis, G., *Heterocycles*, 1985, vol. 23, p. 2051. https://doi.org/10.3987/R-1985-08-2051
8. Farghaly, T.A., Gomha, S.M., Sayed, A.R., and Khedr, M.A., *Curr. Org. Synth*., 2016, vol. 13, p. 445. https://doi.org/10.2174/1570179412666150817220018
9. Shawali, A.S., Farghaly, T.A., and Nawar, T.M.S., *J. Heterocycl. Chem*., 2016, vol. 53, p. 909. https://doi.org/10.1002/jhet.2151
10. Kassem, A.F., Alshehrei, F., Abbas, E.M.H., and Farghaly, T.A., *Mini-Rev. Med. Chem*., 2020, vol. 20, p. 418. https://doi.org/10.2174/1389557519666190603091101
11. Farghaly, T.A., Abdallah, M.A., and Muhammad, Z.A., *Curr. Org. Synth*., 2016, vol. 13, p. 291. https://doi.org/10.2174/1570179412666150706183544
12. Farghaly, T.A., Abdallah, M.A., Masaret, G.S.,and Muhammad, Z.A., *Eur. J. Med. Chem*., 2015, vol. 97, p. 320. https://doi.org/10.1016/j.ejmech.2015.05.009
13. Farghaly, T.A. and Mahmoud, H.K., *J. Heterocycl. Chem*., 2015, vol. 52, p. 86. https://doi.org/10.1002/jhet.1985
14. Abdel Hafez, N.A., Farghaly, T.A., Al-Omar, M.A., and Abdalla, M.M., *Eur. J. Med. Chem*., 2010, vol. 45, p. 4838. https://doi.org/10.1016/j.ejmech.2010.07.053

15. Shawali, A.S. and Farghaly, T.A., *Arkivoc*, 2008, vol. 2008, part (i), p. 18. www.arkat-usa.org/get-file/23038/
16. Farghaly, T.A. and Mahmoud, H.K., *Arch. Pharm. (Weinheim, Ger.)*, 2013, vol. 346, p. 392. https://doi.org/10.1002/ardp.201200486
17. Dawood, K.M., *Tetrahedron*, 2005, vol. 61, p. 5229. https:// doi.org/10.1016/j.tet.2005.03.083
18. Riyadh, S.M. and Farghaly, T.A., *Tetrahedron*, 2012, vol. 68, p. 9056. https://doi.org/10.1016/j.tet.2012.08.064
19. Hakkou, Z., Maciuk, A., Leblais, V., Bouanani, N.E., Mekhfi, H., Bnouham, M., Aziz, M., Ziyyat, A., Rauf, A., Ben Hadda, T., Shaheen, U., Patel, S., Fischmeiste, R., and Legssyer, A., *Biomed. Pharmacother*., 2017, vol. 93, p. 62. https://doi.org/10.1016/j.biopha.2017.06.015
20. Rauf, A., Uysal, S., Ben Hadda, T., Siddiqui, B.S., Khan, H., Atif Khan, M., Ijaz, M.I., Mubarak, M.S., Bawazeer, S., Abu-Izneid, T., Khan, A., and Farooq, U., *Marmara Pharm. J*., 2017, vol. 21, p. 261. https://doi.org/10.12991/marupj.300335
21. Genc, M., Karagoz Genc, Z., Tekin, S., Sandal, S., Sirajuddin, M., and Ben Hadda, T., *Acta Chim. Slov*., 2016, vol. 63, p. 726. https://doi.org/10.17344/acsi.2016.2428
22. Mabkhot, Y.N., Arfan, M., Zgou, H., Genc, Z.K., Genc, M., Rauf, A., Bawazeer, S., and Ben Hadda, T. *Res. Chem. Intermed*., 2016, vol. 42, p. 8055. https://doi.org/10.1007/s11164-016-2578-8
23. Rauf, A., Uddin, G., Siddiqui, B.S., Khan, H., Mujeeb-ur-Rehman, Warad, I., Ben Hadda, T., Patel, S., Khan, A., and Farooq, U., *Curr. Bioactive Compd*., 2015, vol. 11, p. 231. https://doi.org/10.2174/1573407211666151012191902
24. Mabkhot, Y.N., Alatibi, A., El-Sayed, N., Kheder, N., Wadood, A., Rauf, A., Bawazeer, S., Al-Showiman, S., and Ben Hadda, T., *Molecules*, 2016, vol. 21, p. 222. https://doi.org/10.3390/molecules21020222
25. Tatar, E., Şenkardeş, S., Sellitepe, H.E., Güniz Küçükgüzel, Ş., Karaoğlu, S.A., Bozdeveci, A., De Clercq, E., Pannecouque, C., Ben Hadda, T., and Küçükgüzel, İ., *Turk. J. Chem*., 2016, vol. 40, p. 510. https://doi.org/10.3906/kim-1509-21
26. Al-Maqtari, H.M., Jamalis, J., Ben Hadda, T., Sankaranarayanan, M., Chander, S., Ahmad, N.A., Sirat, H.M., Althagafi, I.I., and Mabkhot, Y.N., *Res. Chem. Intermed*., 2017, vol. 43, p. 1893. https://doi.org/10.1007/s11164-016-2737-y
27. Sajid, Z., Ahmad, M., Aslam, S., Ashfaq, U.A., Zahoor, A.F., Saddique, F.A., Parvez, M., Hameed, A., Sultan, S., Zgou, H., and Ben Hadda, T., *Pharm. Chem. J*., 2016, vol. 50, p. 172. https://doi.org/10.1007/s11094-016-1417-y
28. Amirkhanov, V., Rauf, A., Ben Hadda, T., Ovchynnikov, V., Trush, V., Saleem, M., Raza, M., Rehman, T., Zgou, H., Shaheen, U., and Farghaly, T.A., *Mini-Rev. Med. Chem*., 2019, vol. 19, p. 1015. https://doi.org/10.2174/1389557519666190222172757
29. Pervez, H., Ahmad, M., Ben Hadda, T., Toupet, L., and Naseer, M.M., *J. Mol. Struct*., 2015, vol. 1098, p. 124. https://doi.org/10.1016/j.molstruc.2015.06.013
30. Abdelhady, M.I.S., Kamal, A.M., Rauf, A., Mubarak, M.S., and Ben Hadda, T., *Nat. Prod. Res*., 2016, vol. 30, p. 1131. https://doi.org/10.1080/14786419.2015.1045508
31. Header, E., El-Sawy, N., El-Boshy, M., Basalamah, M., Mubarak, M.S., and Ben Hadda, T., *J. Bioanal. Biomed*., 2016, vol. 15, p. 18. https://doi.org/10.4172/1948-593X.1000118
32. Ben Hadda, T., Genc, Z.K., Masand, V.H., Nebbache, N., Warad, I., Jodeh, S., Genc, M., Mabkhot, Y.N., Barakat, A., and Salgado-Zamora, H., *Acta Chim. Slov*., 2015, vol. 62, p. 679. https://doi.org/10.17344/acsi.2015.1357
33. Hatzade, K., Sheikh, J., Taile, V., Ghatole, A., Ingle, V., Genc, M., Lahsasni, S., and Ben Hadda, T., *Med. Chem. Res*., 2015, vol. 24, p. 2679. https://doi.org/10.1007/s00044-015-1326-8
34. Lipinski, C.A., Lombardo, F., Dominy, B.W., and Feeney, P.J., *Adv. Drug Delivery Rev*., 2001, vol. 46, p. 3. https://doi.org/10.1016/S0169-409X(00)00129-0
35. Kaugars, G., Gemrich, E.G., and Rizzo, V.L., *J. Agric. Food Chem*., 1973, vol. 21, p. 647. https://doi.org/10.1021/jf60188a051
36. Hassaneen, H.M., Mousa, H.A.H., Abed, N.M., and Shawali, A.S., *Heterocycles*, 1988, vol. 27, p. 695. https://doi.org/10.3987/COM-87-4381
37. Shawali, A.S. and Albar, H.A., *Can. J. Chem*., 1986, vol. 64, p. 871. https://doi.org/10.1139/v86-144
38. Becke, A.D., *Phys. Rev. A*, 1988, vol. 38, p. 3098. https://doi.org/10.1103/PhysRevA.38.3098
39. Becke, A.D., *J. Chem. Phys*., 1993, vol. 98, p. 5648. https://doi.org/10.1063/1.464913
40. Arjunan, V., Suja Ravi Isaac, A., Rani, T., Mythili, C.V., and Mohan, S., *Spectrochim. Acta, Part A*, 2011, vol. 78, p. 1625. https://doi.org/10.1016/j.saa.2011.02.018
41. Lee, C., Yang, W., and Parr, R.G., *Phys. Rev. B*, 1988, vol. 37, p. 785. https://doi.org/10.1103/PhysRevB.37.785
42. McLean, A.D. and Chandler, G.S., *J. Chem. Phys*., 1980, vol. 72, p. 5639. https://doi.org/10.1063/1.438980
43. Krishnan, R., Binkley, J.S., Seeger, R., and Pople, J.A., *J. Chem. Phys*., 1980, vol. 72, p. 650. https://doi.org/10.1063/1.438955
44. Frisch, M.J., Trucks, G.W., Schlegel, H.B., Scuseria, G.E., Robb, M.A., Cheeseman, J.R., Scalmani, G., Barone, V., Mennucci, B., Petersson, G.A.,

Nakatsuji, H., Caricato, M., Li, X., Hratchian, H.P., Izmaylov, A.F., Bloino, J., Zheng, G., Sonnenberg, J.L., Hada, M., Ehara, M., Toyota, K., Fukuda, R., Hasegawa, J., Ishida, M., Nakajima, T., Honda, Y., Kitao, O., Nakai, H., Vreven, T., Montgomery, J.A., Jr., Peralta, J.E., Ogliaro, F., Bearpark, M., Heyd, J.J., Brothers, E., Kudin, K.N., Staroverov, V.N., Keith, T., Kobayashi, R., Normand, J., Raghavachari, K., Rendell, A., Burant, J.C., Iyengar, S.S., Tomasi, J., Cossi, M., Rega, N., Millam, J.M., Klene, M., Knox, J.E., Cross, J.B., Bakken, V., Adamo, C., Jaramillo, J., Gomperts, R., Stratmann, R.E., Yazyev, O., Austin, A.J., Cammi, R., Pomelli, C., Ochterski, J.W., Martin, R.L., Morokuma, K., Zakrzewski, V.G., Voth, G.A., Salvador, P., Dannenberg, J.J., Dapprich, S., Daniels, A.D., Farkas, O., Foresman, J.B., Ortiz, J.V., Cioslowski, J., and Fox, D.J., *Gaussian 09W*, Wallingford CT: Gaussian, 2010.

45. Dennington, R., Keith, T., and Millam, J., *Gauss View,* version 5, Shawnee Mission KS: Semichem, 2009.

46. Vijayan, P., Raghu, C., Ashok, G., Dhanaraj, S.A., and Suresh, B., *Indian J. Med. Res*., 2004, vol. 120, p. 24.